Computer Assisted Mechanics and Engineering Sciences, 5: 161–172, 1998.
Copyright © 1998 by Polska Akademia Nauk

Absolute instabilities of a finite length vortex street with external axial velocities

Tak Wai Chiu and Aaron Hanson Berney
School of Engineering
University of Exeter
Exeter EX4 4QF, UK

(Received January 24, 1997)

This paper presents a numerical algorithm for the study of the absolute instability of a vortex street with external axial velocities and finite length vortices. The aim is that this will be of relevance to the study of the flow over slender bodies at yaw. The algorithm is based on the vortex dynamics momentum equation. Special core treatments have been implemented to tackle the problem of infinite self-induced velocity. A small perturbation method is then used to formulate the eigenvalue problem.

1. INTRODUCTION

The present work began as part of our research into the stability of the vortex wake behind slender bodies at yaw. The flow over slender bodies has been the subject of a large number of research projects since the beginning of this century due to its relevance to the dynamics of missiles, rockets, submarines and railway trains, and its intrinsic complexity. The flow regime around a slender body can be divided into three main categories which depends greatly on the yaw angles.

Consider a missile-like slender circular cylinder at yaw as shown in Fig. 1. At very small yaw angles below, approximately, 10°, the fluid flows round the body very smoothly without any flow separation.

At yaw angles above 10°, flow separation occurs on the leeside of the body and the wake is characterised by the two rows of steady line-vortices (vortex filaments) as shown in Fig. 1 which resembles a three-dimensional vortex street. This steady vortex wake is the most characteristic flow

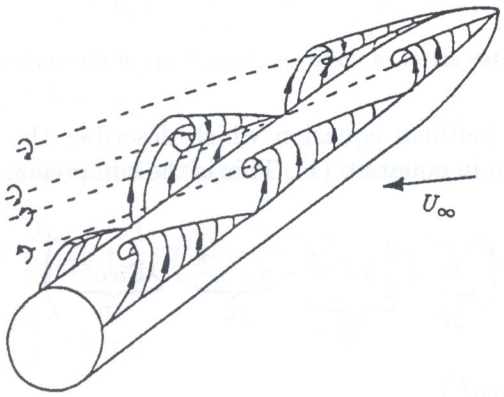

Fig. 1. The steady vortex wake behind a slender body at yaw.

regime and is usually called the slender body flow structure. If one looks at the cross-section of the flow structure at various distances from the nose, one can see that the development of the wake in the lengthwise direction is similar to the time variation of the wake in the impulsively started flow over a circular cylinder. This similarity is usually called the cross-flow analogy.

At yaw angles above 60°, instability is observed and the steady vortex structure breaks down into a vortex shedding regime. This behaviour has been observed experimentally by many researchers, for example by Chiu and Squire [1], Degani and Zilliac [2] and Zilliac et al [3]. They observed pressure fluctuations corresponding to vortex shedding ocurring at an angle of incidence of 85°, but not at 50°. The aim of the research presented in this paper is to analyse the stability of the steady vortices in the hope that this will shed some light on the mechanism of break up of the steady vortex pattern.

2. THE GOVERNING EQUATION

In the present analysis, we begin with the modified form of the Moore–Saffman equation [4]. The vortex street contains a number of finite length vortices as shown in Fig. 2 and each vortex is modelled as a number of straight line vortex segments. The influence of the movement of the nodes upon all the other nodal velocities is linearised and expressed in matrix form. Convective and absolute instabilities can be investigated from this matrix [5]. In order to effectively model the self-induced velocity of a vortex, a vortex core treatment is required. In an ideal inviscid vortex, the vorticity is zero everywhere except at the centre of the vortex, where it is infinite. In the present model, we adopt a uniform core: the vorticity is finite and constant within the core, and zero without.

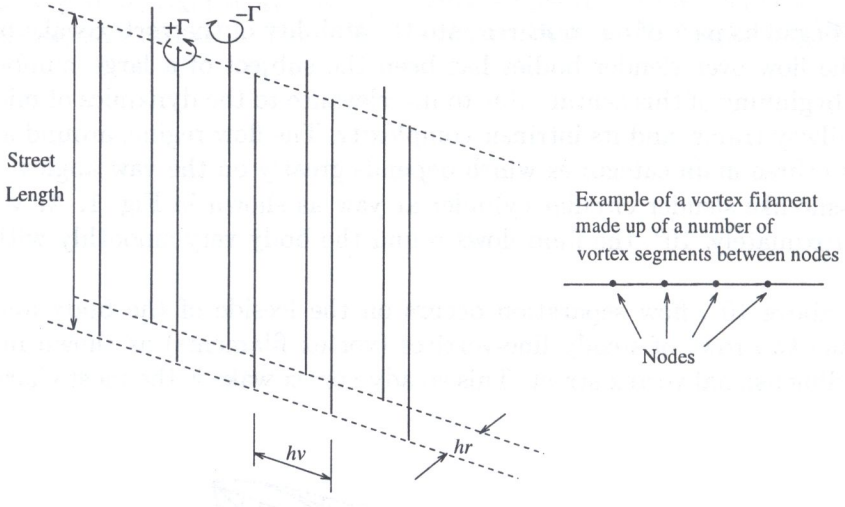

Fig. 2. A vortex street of finite length and one of the vortex filaments.

We began with the Moore–Saffman equation which describes the dynamics of a vortex with internal axial velocities is shown in equation (1). This is the component of the momentum equation perpendicular to $\hat{s}$

$$\underbrace{\Gamma\left(\vec{V}_E+\vec{V}_I-\frac{\partial\vec{R}}{\partial t}\right)\times\hat{s}}_{\text{I}}+\frac{\hat{n}}{\rho}\Bigg(\underbrace{T_0}_{\text{II}}+\underbrace{\frac{1}{2}\pi a^2\overline{v^2}}_{\text{III}}-\underbrace{\pi a^2\overline{w^2}}_{\text{IV}}+\underbrace{\lambda\Gamma\overline{w}a^2\tau}_{\text{V}}\Bigg)$$

$$-\underbrace{2\pi a^2\overline{w}\frac{\partial\hat{s}}{\partial t}}_{\text{VI}}-\underbrace{\vec{b}\Gamma\frac{\partial}{\partial s}\left(\frac{\lambda\overline{w}a^2}{\rho}\right)}_{\text{VII}}=0\,. \tag{1}$$

Readers who are interested in the derivation of this equation should refer to Moore and Saffman [4]. Here only a brief description of the terms involved in equation (1) will be given. The term 'external' is used to refer to 'outside of the core' while the term 'internal' describes what is going on 'within the core'. Term I is the external force term related to the induced velocity due to the movement of the vortex filament. This force term is sometimes called the Kutta force. Term II, the tension, is an external force term which appear when the filament is curved. The swirling flow around the core is distorted and the flow velocities are slightly increased on the concave side and slightly decreased on the convex side of the filament. The resultant changes in the pressure field cause a force, $T_0\hat{\mathrm{n}}/\rho$, on the vortex towards the centre of curvature. Term III to VII are internal force terms related to the fluid motion within the core. Term III is similar to term II. It is the result of tension caused by the curvature and swirling motion within the core. Terms IV, VII, V and half of term VI are the Reynolds stress contributions. The other half of term VI is the contribution due to the rate of change of momentum of the core fluid.

Equation (1) can be manipulated to a form more suitable for our studies. First, terms V and VII will be dealt with together

$$\frac{\hat{\mathrm{n}}}{\rho}\lambda\Gamma\overline{w^2}\tau - \vec{\mathrm{b}}\Gamma\frac{\partial}{\partial s}\left(\frac{\lambda\overline{w}a^2}{\rho}\right) = \lambda\Gamma a^2\overline{w}\left(\frac{\hat{\mathrm{n}}\tau}{\rho} - \vec{\mathrm{b}}\frac{\partial\frac{1}{\rho}}{\partial s}\right) - \frac{\vec{\mathrm{b}}\Gamma}{\rho}\frac{\partial}{\partial s}(\lambda\overline{w}a^2)\,. \tag{2}$$

First it will be assumed that the core profile is uniform along its length, i.e. $\partial(\lambda\overline{w}a^2)/\partial s = 0$. The last term of equation (2) thus vanishes. After some substitutions and rearrangements, the rest of equation (2) becomes

$$\lambda\Gamma a^2\overline{w}\left(\frac{\hat{\mathrm{n}}\tau}{\rho} - \vec{\mathrm{b}}\frac{\partial\frac{1}{\rho}}{\partial s}\right) = \lambda\Gamma a^2\overline{w}\left(\frac{\partial^2\hat{\mathrm{s}}}{\partial s^2}\times\hat{\mathrm{s}}\right)\,. \tag{3}$$

Substituting this back to equation (1) we get

$$\Gamma\left(\vec{\mathrm{V}}_E + \vec{\mathrm{V}}_I - \frac{\partial\vec{\mathrm{R}}}{\partial t}\right)\times\hat{\mathrm{s}} + \frac{\hat{\mathrm{n}}}{\rho}\left(T_0 + \frac{1}{2}\pi a^2\overline{v^2} - \pi a^2\overline{w^2}\right) - 2\pi a^2\overline{w}\frac{\partial\hat{\mathrm{s}}}{\partial t} + \lambda\Gamma a^2\overline{w}\frac{\partial^2\hat{\mathrm{s}}}{\partial s^2}\times\hat{\mathrm{s}} = 0\,. \tag{4}$$

The next modification concerns the fact that the original Moore–Saffman equation applies only for cases where there is no external axial velocity. In other words, the equation will apply only when the frame of reference upon which s is based moves at the same speed as the external axial velocity field. To allow the equation to deal with external axial velocities the derivatives with respect to time must be modified to include the convective terms. Now to obtain the Moore–Saffman equation based on a fixed frame of reference, we will

$$\text{replace}\quad \frac{\partial\vec{\mathrm{R}}}{\partial t}\quad\text{by}\quad \frac{\partial\vec{\mathrm{R}}}{\partial t} - [(\vec{\mathrm{V}}_E + \vec{\mathrm{V}}_I)\cdot\hat{\mathrm{s}}]\frac{\partial\vec{\mathrm{R}}}{\partial s} = \frac{\partial\vec{\mathrm{R}}}{\partial t} - [(\vec{\mathrm{V}}_E + \vec{\mathrm{V}}_I)\cdot\hat{\mathrm{s}}]\hat{\mathrm{s}}$$

$$\text{and}\quad \frac{\partial\hat{\mathrm{s}}}{\partial t}\quad\text{by}\quad \frac{\partial\hat{\mathrm{s}}}{\partial t} - [(\vec{\mathrm{V}}_E + \vec{\mathrm{V}}_I)\cdot\hat{\mathrm{s}}]\frac{\partial\hat{\mathrm{s}}}{\partial s}\,.$$

Putting everything together, the modified form of the Moore–Saffman equation is obtained:

$$\Gamma\left(\vec{\mathrm{V}}_E + \vec{\mathrm{V}}_I - \frac{\partial\vec{\mathrm{R}}}{\partial t}\right)\times\hat{\mathrm{s}} + \frac{\partial\hat{\mathrm{s}}}{\partial s}[T_0 + \frac{1}{2}\pi a^2\overline{v^2} - \pi a^2\overline{w^2} + 2\pi a^2\overline{w}(\vec{\mathrm{V}}_E + \vec{\mathrm{V}}_I)\cdot\hat{\mathrm{s}}]$$
$$-2\pi a^2\overline{w}\frac{\partial\hat{\mathrm{s}}}{\partial t} + \lambda\Gamma a^2\overline{w}\frac{\partial^2\hat{\mathrm{s}}}{\partial s^2}\times\hat{\mathrm{s}} = 0\,. \tag{5}$$

The next step is to evaluate the tension term T_0. This must be determined in conjunction with $\vec{\mathrm{V}}_I$. Moore and Saffman suggested the use of an osculating vortex ring (see [4]). The idea is that if we consider the velocity at a point, say P, on the vortex filament due to this filament itself, we

can calculate the induced velocity in a straight forward manner using the Biot–Savart law up to a certain small distance, d either side of P. Within this distance from P, the effect of the vortex core must be taken into account in order to obtain a realistic induced velocity. To model that, we first evaluate the tension term as if we were doing it for a vortex ring (let us call it the *first vortex ring*) with core radius a and ring radius ρ equal to the local radius of curvature. Then the effect of an open vortex ring (the *second vortex ring*) of the opposite strength and a cut-off distance d is added to cancel the effect of most of the first vortex ring. For this method, they determined that

$$T_0 = \frac{\Gamma^2}{4\pi}\left(\log\frac{8\rho}{a} - \frac{1}{2}\right). \tag{6}$$

The question arises as to how we should calculate the self induced velocity $\vec{\mathrm{V}}_I$ with such an osculating vortex ring for a vortex modelled using straight line vortex segments. In the present study, the vortex filament modelled are all made up of a number of segments. Therefore, to evaluate $\vec{\mathrm{V}}_I$ the velocity induced by the vortex with cut-off and the velocity induced by the osculating vortex ring of strength $-\Gamma$ also with cut-off (the second vortex ring) must be added together.

The magnitude of the velocity of self propagation of a vortex ring with a small cut-off distance d, vortex strength $-\Gamma$ and ring radius ρ is given by

$$-\frac{\Gamma}{4\pi\rho}\log\left(\frac{4\rho}{d}\right), \tag{7}$$

provided that $d \ll \rho$. The velocity induced is in the direction, $\vec{\mathrm{b}}$, perpendicular to the plane of the ring. In this way, $\vec{\mathrm{V}}_E$ and $\vec{\mathrm{V}}_I$ can be grouped together. Here the term $\vec{\mathrm{V}}_c$ is the induced velocity due to all the vortex segments on all filaments, with a cut-off distance on the self-inducing filament.

$$\vec{\mathrm{V}}_E + \vec{\mathrm{V}}_I = \vec{\mathrm{V}}_c - \frac{\Gamma\vec{\mathrm{b}}}{4\pi\rho}\log\left(\frac{4\rho}{d}\right). \tag{8}$$

Substituting (8) into (5), and after some simplifications the following governing equation is obtained:

$$\dot{\vec{\mathrm{R}}}\times\hat{\mathrm{s}} + \frac{2\pi a^2\overline{w}}{\Gamma}\dot{\hat{\mathrm{s}}} = \vec{\mathrm{V}}_c\times\hat{\mathrm{s}} + \frac{\partial\hat{\mathrm{s}}}{\partial s}\left(C + \frac{2\pi a^2\overline{w}}{\Gamma}\vec{\mathrm{V}}_c\cdot\hat{\mathrm{s}}\right) + \lambda a^2\overline{w}\frac{\partial^2\hat{\mathrm{s}}}{\partial s^2}\times\hat{\mathrm{s}}, \tag{9}$$

in which

$$C = \frac{\Gamma}{4\pi}\left[\log\left(\frac{2d}{a}\right) - \frac{1}{2}\right] + \frac{1}{2}\pi a^2\overline{v^2} - \pi a^2\overline{w^2}. \tag{10}$$

If terms of order $(a/\rho)^2$ are neglected, equation (9) becomes

$$\dot{\vec{\mathrm{R}}}\times s = \vec{\mathrm{V}}_c\times\hat{\mathrm{s}} + C\frac{\partial\hat{\mathrm{s}}}{\partial s}. \tag{11}$$

3. THE CUT-OFF DISTANCE

The cut-off distance, d, is only concerned with minimising computational error. If d is too small relative to the vortex segment lengths, then the discretisation of the vortex into straight line segments will entail poor calculation of the velocity induced by the closest vortex segments beyond the cut-off. Indeed, since the vortex segments are straight, if the cut-off distance is less than the distance to the end of the segment, the remainder of the segment will not induce any velocity. Hence such a small cut-off distance has no meaning. If however the cut-off distance is set to too large a value relative to the features of the vortex filament geometry, the cut-off will remove geometric features of the vortex filament close to the observation point. The compromised value of d in the present calculation is chosen as 2 vortex segment lengths.

4. Evaluating the curvature

Since in this algorithm the vortex filaments are discretised into straight line vortex segments, it is necessary to determine an approximate curvature vector, $\vec{\mathrm{q}}$ (the numerical approximation of $\hat{\mathrm{n}}/\rho$, note that $\hat{\mathrm{n}}/\rho$ is equal to $\partial\hat{\mathrm{s}}/\partial s$) from the nodal coordinates. Using the Galerkin method we obtain the following weak formulation. Linear weighting function, W, is used, i.e. W varies from 0 at one end node of the vortex segment to 1 at the the other end node. The integration is over the two segments connected to a node.

$$\int \left(\vec{\mathrm{q}} - \frac{\partial\hat{\mathrm{s}}}{\partial s}\right) W \mathrm{d}s = 0\,. \tag{12}$$

Noting that the weighting functions are only non-zero for the two segments on either side of a particular node, and using the node numbers to refer to the integral domain, we can say that, for a general function $f(s)$

$$\int f(s) W_n \mathrm{d}s = \int_{n-1}^{n} f(s) W_n \mathrm{d}s + \int_{n}^{n+1} f(s) W_n \mathrm{d}s\,. \tag{13}$$

Given that the curvature is zero over the length of each segment, the integral of $W(\partial\hat{\mathrm{s}}/\partial s)$ for each node is simply the change in the unit parallel vector from the lowered numbered segment to the higher. With linear shape function for $\vec{\mathrm{q}}$, the vector equation for curvature at node n is thus:

$$\frac{\ell_{n-1}}{6}(\vec{\mathrm{q}}_{n-1} + 2\vec{\mathrm{q}}_n) + \frac{\ell_n}{6}(2\vec{\mathrm{q}}_n + \vec{\mathrm{q}}_{n+1}) - (\hat{\mathrm{s}}_n - \hat{\mathrm{s}}_{n-1}) = 0\,, \tag{14}$$

in which $\hat{\mathrm{s}}_n$ and $\hat{\mathrm{s}}_{n-1}$ are the unit vectors parallel to the n^{th} and the $(\mathrm{n}\text{-}1)^{\mathrm{th}}$ segments. $\hat{\mathrm{s}}_n$ is calculated using $\hat{\mathrm{s}}_n = (\vec{\mathrm{R}}_{n+1} - \vec{\mathrm{R}}_n)/\ell_n = (\Delta\vec{\mathrm{R}})_n/\ell_n$. The approximated curvatures $\vec{\mathrm{q}}_n$ at each node can thus be obtained from the nodal coordinates by solving a system of linear equations. It will be seen that the determination of the curvature is only important when second order terms are taken into account.

5. Discretising the vortex dynamics governing equation

Once the curvature is available as an independent variable, the governing equation can be re-written as

$$\dot{\vec{\mathrm{R}}} \times \hat{\mathrm{s}} + \frac{2\pi a^2 \overline{w}}{\Gamma}\dot{\hat{\mathrm{s}}} = \vec{\mathrm{V}}_c \times \hat{\mathrm{s}} + \frac{\partial\hat{\mathrm{s}}}{\partial s}\left(C + \frac{2\pi a^2 \overline{w}}{\Gamma}\vec{\mathrm{V}}_c \cdot \hat{\mathrm{s}}\right) + \lambda a^2 \overline{w}\frac{\partial\vec{\mathrm{q}}}{\partial s} \times \hat{\mathrm{s}}\,. \tag{15}$$

The next task is to carry out the discretisation process by evaluating the integrals over the domain of each segment for each of the weighting functions. Though it is not explicitly implemented, axial convection arises in the governing equation, and therefore upwinding must be used to prevent oscillatory solutions. This involves modifying the weighting functions to W'. The Petrov-Galerkin procedure presented in Zienkiewicz and Taylor [6] is employed:

$$W'_n = W_n + \frac{\alpha\ell}{2}\frac{\mathrm{d}W_n}{\mathrm{d}s}\,. \tag{16}$$

For the weighting functions used here this gives

$$\begin{aligned} W'_n &= W_n + \frac{1}{2}\alpha, \quad (\mathrm{n}\text{-}1)^{\mathrm{th}} \text{ segment;} \\ &= W_n - \frac{1}{2}\alpha, \quad \mathrm{n}^{\mathrm{th}} \text{ segment} \end{aligned}$$

α being the upwinding factor. It is found that the optimum value of α is a tensor, $[\alpha]$. Hence the weighting function itself is also a tensor, $[W]_n$ etc.

$$\begin{aligned}[W]_n &= [I]W_n + \frac{1}{2}[\alpha], \quad \text{(n-1)}^{\text{th}} \text{ segment;} \\ &= [I]W_n - \frac{1}{2}[\alpha], \quad \text{n}^{\text{th}} \text{ segment,}\end{aligned}$$

in which $[I]$ is the unit tensor. The "prime" has been left off since it avoids confusion with those associated with small perturbation to be discussed later. The integral form of the governing equation becomes

$$\begin{aligned}\int \left(\dot{\vec{\mathrm{R}}} \times \hat{\mathrm{s}}\right)[W]_n \mathrm{d}s + \frac{2\pi a^2 \overline{w}}{\Gamma} \int \dot{\hat{\mathrm{s}}}[W]_n \mathrm{d}s &= \int (\vec{\mathrm{V}}_c \times \hat{\mathrm{s}})[W]_n \mathrm{d}s + C \int \frac{\partial \hat{\mathrm{s}}}{\partial s}[W]_n \mathrm{d}s \\ + \frac{2\pi a^2 \overline{w}}{\Gamma} \int \left(\vec{\mathrm{V}}_c \cdot \hat{\mathrm{s}} \frac{\partial \hat{\mathrm{s}}}{\partial s}\right)[W]_n \mathrm{d}s + \lambda a^2 \overline{w} \int \left(\frac{\partial \vec{\mathrm{q}}}{\partial s} \times \hat{\mathrm{s}}\right)[W]_n \mathrm{d}s\,. &\end{aligned} \tag{17}$$

The terms involving $\vec{\mathrm{V}}_c$ must be evaluated numerically, and will be carried out later. The discretisation of the terms not involving $\vec{\mathrm{V}}_c$ is presented below. Please note the following notation. From $\hat{\mathrm{s}}_n = (\Delta\vec{\mathrm{R}})_n/\ell_n$, we can express $\dot{\hat{\mathrm{s}}}_n$ as

$$\dot{\hat{\mathrm{s}}}_n = \frac{1}{\ell_n}(\Delta\dot{\vec{\mathrm{R}}})_n - \frac{\hat{\mathrm{s}}_n}{\ell_n}(\Delta\dot{\vec{\mathrm{R}}})_n \cdot \hat{\mathrm{s}}_n = \frac{1}{\ell_n}(\Delta\dot{\vec{\mathrm{R}}})_n\{[I] - \hat{\mathrm{s}}_n; \hat{\mathrm{s}}_n\}\,, \tag{18}$$

in which the semi-colon, e.g. $\vec{\mathrm{a}}; \vec{\mathrm{b}}$, signifies the dyadic product of two vectors, the result of which is a second order tensor, say $[D]$, such that $D_{ij} = a_i b_j$. The value of $\dot{\hat{\mathrm{s}}}_n$ is constant along the segment and therefore the integration is trivial:

$$\int \dot{\hat{\mathrm{s}}}[W]_n \mathrm{d}s = (\Delta\dot{\vec{\mathrm{R}}})_{n-1}\{[I] - \hat{\mathrm{s}}_{n-1}; \hat{\mathrm{s}}_{n-1}\}\left(\frac{[I] + [\alpha]}{2}\right) + (\Delta\dot{\vec{\mathrm{R}}})_n\{[I] - \hat{\mathrm{s}}_n; \hat{\mathrm{s}}_n\}\left(\frac{[I] - [\alpha]}{2}\right). \tag{19}$$

Similarly, $\partial\vec{\mathrm{q}}/\partial s$ has a constant value of $(\Delta\vec{\mathrm{q}})_n/\ell_n$, giving

$$\int \left(\frac{\partial \vec{\mathrm{q}}}{\partial s} \times \hat{\mathrm{s}}\right)[W]_n \mathrm{d}s = ((\Delta\vec{\mathrm{q}})_{n-1} \times \hat{\mathrm{s}}_{n-1})\left(\frac{[I] + [\alpha]}{2}\right) + ((\Delta\vec{\mathrm{q}})_n \times \hat{\mathrm{s}}_n)\left(\frac{[I] - [\alpha]}{2}\right). \tag{20}$$

The next term is discretised by assuming that the values of the weighting function at the nodes are unchanged by the implementation of upwinding. Hence,

$$\int \frac{\partial \hat{\mathrm{s}}}{\partial s}[W]_n \mathrm{d}s = \hat{\mathrm{s}}_n - \hat{\mathrm{s}}_{n-1}\,. \tag{21}$$

Finally, $\dot{\vec{\mathrm{R}}}$ varies linearly over the segments, giving

$$\begin{aligned}\int \left(\dot{\vec{\mathrm{R}}} \times \hat{\mathrm{s}}\right)[W]_n \mathrm{d}s = &\frac{1}{6}\left(\dot{\vec{\mathrm{R}}}_{n-1} + 2\dot{\vec{\mathrm{R}}}_n\right) \times (\Delta\vec{\mathrm{R}})_{n-1} + \frac{1}{6}\left(2\dot{\vec{\mathrm{R}}}_n + \dot{\vec{\mathrm{R}}}_{n+1}\right) \times (\Delta\vec{\mathrm{R}})_n \\ &+ \frac{1}{2}\left\{\left(\dot{\vec{\mathrm{R}}}_{n-1} + \dot{\vec{\mathrm{R}}}_n\right) \times (\Delta\vec{\mathrm{R}})_{n-1} - \left(\dot{\vec{\mathrm{R}}}_n + \dot{\vec{\mathrm{R}}}_{n+1}\right) \times (\Delta\vec{\mathrm{R}})_n\right\}[\alpha]\,.\end{aligned} \tag{22}$$

6. Evaluation of the terms involving $\vec{\mathrm{V}}_C$

The velocity induced by the vortex segments, $\vec{\mathrm{V}}_c$, can be evaluated at any point, by integrating the Biot–Savart law. Since the vortex is made up of straight line segments, this can be done by summation of the velocity due to each segment. The velocity at a point p induced by the m^{th} straight line vortex segment of strength Γ running from $\vec{\mathrm{R}}_m$ to $\vec{\mathrm{R}}_{m+1}$ is given by

$$\vec{\mathrm{U}}_{p,m} = \frac{\Gamma}{4\pi} \frac{\vec{\mathrm{X}}_1 \times \vec{\mathrm{X}}_2}{fh - g^2}\left(\frac{h - g}{\sqrt{h}} + \frac{f - g}{\sqrt{f}}\right), \tag{23}$$

in which

$$\vec{X}_1 = \vec{R}_m - \vec{R}_p\,, \quad \vec{X}_2 = \vec{R}_{m+1} - \vec{R}_p \tag{24}$$

and

$$f = \vec{X}_1 \cdot \vec{X}_1\,, \quad g = \vec{X}_1 \cdot \vec{X}_2\,, \quad h = \vec{X}_2 \cdot \vec{X}_2\,. \tag{25}$$

The total induced velocity can then be calculated by summing $\vec{U}_{p,m}$ by taking into account all the vortex segments, excluding those that are within the cut-off distance, i.e.

$$\vec{V}_{c,p} = \sum_m \vec{U}_{p,m}\,, \tag{26}$$

in which $\vec{V}_{c,p}$ is the total induced velocity at the point $\vec{R}_p$. Now the $\vec{V}_c$ terms in equation (17) can be discretised as follows:

$$\begin{aligned}\int (\vec{V}_c \times \hat{s})[W]_n \mathrm{d}s \;=\; & \frac{1}{6}(\vec{V}_{c,n-1} + \vec{V}_{c,n}) \times (\Delta\vec{R})_{n-1} + \frac{1}{6}(2\vec{V}_{c,n} + \vec{V}_{c,n+1}) \times (\Delta\vec{R})_n \\ & + \frac{1}{2}((\vec{V}_{c,n-1} + \vec{V}_{c,n}) \times (\Delta\vec{R})_{n-1} - (\vec{V}_{c,n} + \vec{V}_{c,n+1}) \times (\Delta\vec{R})_n)[\alpha]\,,\end{aligned} \tag{27}$$

$$\int (\vec{V}_c \cdot \hat{s}) \frac{\partial \hat{s}}{\partial s}[W]_n \mathrm{d}s = \vec{V}_{c,n}(\hat{s}_n; \hat{s}_n - \hat{s}_{n-1}; \hat{s}_{n-1})\,. \tag{28}$$

7. Linearisation of the integrals — small perturbation

After the discretisation of the governing integral equation, small perturbation principal is applied to the discretised form of equation (17) and then the tedious but straightforward task of linearisation is carried out by eliminating higher order terms.

7.1. Perturbation to the curvature

In Sec. 4 we have obtained the equation from which the curvatures at the nodes can be computed. When the nodes are given small perturbations, the lengths of the vortex segments will change, causing the nodal curvatures to changes as well. Hence terms like $\vec{q}'_n$ and $(\Delta q')_n$ will appear in the linearised equations. Therefore the perturbation to the nodal curvature due to small nodal displacements must be determined first. This can be achieved by considering the perturbation to equation (14), which yields

$$\begin{aligned}\left(\int \left(\vec{q} - \frac{\partial \hat{s}}{\partial s}\right) W \mathrm{d}s\right)' \;=\; & \left[\frac{\ell_{n-1}}{6}(\vec{q}'_{n-1} + 2\vec{q}'_n) + \frac{\ell_n}{6}(2\vec{q}'_n + \vec{q}'_{n+1})\right] \\ & + \left[\frac{\ell'_{n-1}}{6}(\vec{q}_{n-1} + 2\vec{q}_n) + \frac{\ell'_n}{6}(2\vec{q}_n + \vec{q}_{n+1})\right] \\ & - \left[\frac{(\Delta\vec{R}')_{n-1}}{\ell_{n-1}}\{[I] - \hat{s}_{n-1}; \hat{s}_{n-1}\} + \frac{(\Delta\vec{R}')_n}{\ell_n}\{[I] - \hat{s}_n; \hat{s}_n\}\right] = 0\,.\end{aligned} \tag{29}$$

In this way, as in Sec. 4 the perturbation to the curvature can be determined by solving a system of linear equations. It will be seen in the next section that the curvature is only important when second order terms are taken into account.

7.2. Perturbation to the governing equation

Similar procedure can now be carried out on the discretised form of equation (17).

$$\left(\int\left(\dot{\vec{\mathrm{R}}}\times\hat{\mathrm{s}}\right)[W]_n\mathrm{d}s\right)'+\frac{2\pi a^2\overline{w}}{\Gamma}\left(\int\dot{\hat{\mathrm{s}}}[W]_n\mathrm{d}s\right)'=\left(\int(\vec{\mathrm{V}}_c\times\hat{\mathrm{s}})[W]_n\mathrm{d}s\right)'+C\left(\int\frac{\partial\hat{\mathrm{s}}}{\partial s}[W]_n\mathrm{d}s\right)'$$

$$+\frac{2\pi a^2\overline{w}}{\Gamma}\left(\int\left(\vec{\mathrm{V}}_c\cdot\hat{\mathrm{s}}\frac{\partial\hat{\mathrm{s}}}{\partial s}\right)[W]_n\mathrm{d}s\right)'+\lambda a^2\overline{w}\left(\int\left(\frac{\partial\vec{\mathrm{q}}}{\partial s}\times\hat{\mathrm{s}}\right)[W]_n\mathrm{d}s\right)'. \tag{30}$$

So far we have preserved the generality of the equations by including all the first and second order terms. Indeed the analysis can now be simplified enormous by neglecting terms of order $(a/\rho)^2$. In this case the equation becomes

$$\left(\int\left(\dot{\vec{\mathrm{R}}}\times\hat{\mathrm{s}}\right)[W]_n\mathrm{d}s\right)'=\left(\int(\vec{\mathrm{V}}_c\times\hat{\mathrm{s}})[W]_n\mathrm{d}s\right)'+C\left(\int\frac{\partial\hat{\mathrm{s}}}{\partial s}[W]_n\mathrm{d}s\right)'. \tag{31}$$

The discretised form of the terms in equation (31), as in Sec. 5 can be linearised to give the following expressions:

$$\left(\int\left(\dot{\vec{\mathrm{R}}}\times\hat{\mathrm{s}}\right)[W]_n\mathrm{d}s\right)'=\frac{1}{6}(\dot{\vec{\mathrm{R}}}'_{n-1}+2\dot{\vec{\mathrm{R}}}'_n)\times(\Delta\vec{\mathrm{R}})_{n-1}+\frac{1}{6}(2\dot{\vec{\mathrm{R}}}'_n+\dot{\vec{\mathrm{R}}}'_{n+1})\times(\Delta\vec{\mathrm{R}})_n$$

$$+\frac{1}{2}\left((\dot{\vec{\mathrm{R}}}'_{n-1}+\dot{\vec{\mathrm{R}}}'_n)\times(\Delta\vec{\mathrm{R}})_{n-1}-(\dot{\vec{\mathrm{R}}}'_n+\dot{\vec{\mathrm{R}}}'_{n+1})\times(\Delta\vec{\mathrm{R}})_n\right)[\alpha], \tag{32}$$

$$\left(\int\frac{\partial\hat{\mathrm{s}}}{\partial s}[W]_n\mathrm{d}s\right)'=\frac{(\Delta\vec{\mathrm{R}}')_{n-1}}{\ell_{n-1}}\{[I]-\hat{\mathrm{s}}_{n-1};\hat{\mathrm{s}}_{n-1}\}+\frac{(\Delta\vec{\mathrm{R}}')_n}{\ell_n}\{[I]-\hat{\mathrm{s}}_n;\hat{\mathrm{s}}_n\}, \tag{33}$$

$$\left(\int(\vec{\mathrm{V}}_c\times\hat{\mathrm{s}})[W]_n\mathrm{d}s\right)'=\frac{1}{6}((\vec{\mathrm{V}}'_{c,n-1}+2\vec{\mathrm{V}}'_{c,n})\times(\Delta\vec{\mathrm{R}})_{n-1}+(2\vec{\mathrm{V}}'_{c,n}+\vec{\mathrm{V}}'_{c,n+1})\times(\Delta\vec{\mathrm{R}})_n)$$

$$+\frac{1}{2}((\vec{\mathrm{V}}'_{c,n-1}+\vec{\mathrm{V}}'_{c,n})\times(\Delta\vec{\mathrm{R}})_{n-1}-(\vec{\mathrm{V}}'_{c,n}+\vec{\mathrm{V}}'_{c,n+1})\times(\Delta\vec{\mathrm{R}})_n)[\alpha]$$

$$+\frac{1}{6}((\vec{\mathrm{V}}_{c,n-1}+2\vec{\mathrm{V}}_{c,n})\times(\Delta\vec{\mathrm{R}})'_{n-1}+(2\vec{\mathrm{V}}_{c,n}+\vec{\mathrm{V}}_{c,n+1})\times(\Delta\vec{\mathrm{R}})'_n)$$

$$+\frac{1}{2}((\vec{\mathrm{V}}_{c,n-1}+\vec{\mathrm{V}}_{c,n})\times(\Delta\vec{\mathrm{R}})'_{n-1}-(\vec{\mathrm{V}}_{c,n}+\vec{\mathrm{V}}_{c,n+1})\times(\Delta\vec{\mathrm{R}})'_n)[\alpha]. \tag{34}$$

Assuming that each node (take the m^{th} node, $\vec{\mathrm{R}}_m$, as an example) has two degrees of freedom in the directions $\hat{\mathrm{d}}_{1,m}$ and $\hat{\mathrm{d}}_{2,m}$, such that $\vec{\mathrm{R}}'_m=x'_{2m}\hat{\mathrm{d}}_{1,m}+x'_{2m+1}\hat{\mathrm{d}}_{2,m}$, after some lengthy but straight forward manipulations, an eigenvalue problem of the following form is obtained

$$[B_{ij}](\dot{x}'_j)=[A_{ij}](x'_j), \tag{35}$$

in which $[B_{ij}]$ and $[A_{ij}]$ are n×n matrices (n= 2×the number of nodes). From this equation the absolute stabilities of the system of vortices can be investigated. If the disturbance assumes the form

$$\begin{pmatrix}x'_1\\x'_2\\\vdots\\x'_n\end{pmatrix}=\begin{pmatrix}X'_1\\X'_2\\\vdots\\X'_n\end{pmatrix}e^{rt}, \tag{36}$$

in which the X's are the moduli and r is complex, we will end up with an eigenvalue problem such that

$$r[B_{ij}](X'_j)=[A_{ij}](X'_j), \tag{37}$$

in which r is the complex eigenvalue to be determined. The system will be stable if the real parts of all the eigenvalues are non-positive.

8. THE VORTEX STREET AND THE RESULTS

To investigate the absolute stabilities of a vortex street as in Fig. 2 under the influence of an external axial flow using the above results, we face the problem that there are an infinite number of vortex filaments involved. A number of tests have thus been carried out to see whether a finite number of vortex filaments can suffice. It is found that when there are more than 10 vortices, the results will change very little with respect to further increase in the number of vortices. The results presented here have been obtained using a vortex street containing 20 vortices. The number of vortex segments in each vortex filament is not an influencial parameter. The results presented here have been obtained for 20 segments per vortex filament.

As stated in the previous section, the solution to the eigenvalue problem in equation (37) can reveal the stability of the vortex system. If the real parts of all the eigenvalues, r, are negative, then the system is stable because the perturbations are attenuated with respect to time.

Figures 3, 4 and 5 present the effects of the axial velocity, w, the street length, the spacing ratio, h_r/h_v, and the core radius. It was found that for a given street length, the axial velocity has to be greater than a certain critical value for the vortex street to be stable. The graphs are thus plotted to show the values of the axial velocity above which the vortex street is stable.

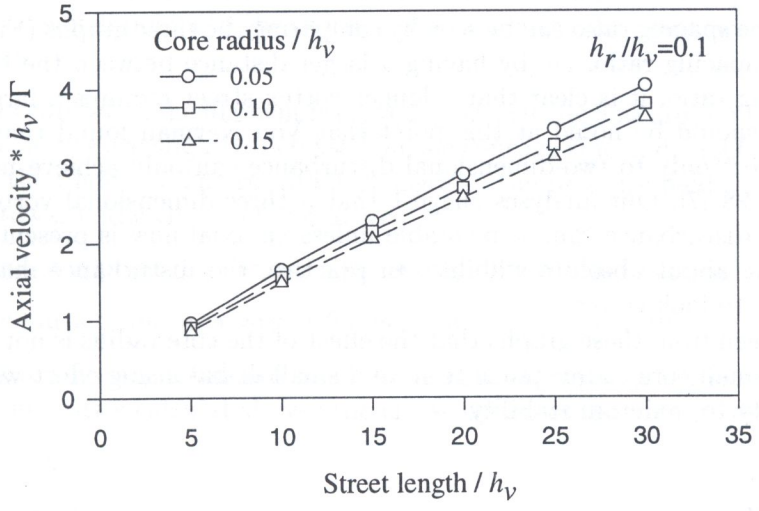

Fig. 3. Minimum axial velocity to maintain stability of vortex street, $h_r/h_v = 0.1$.

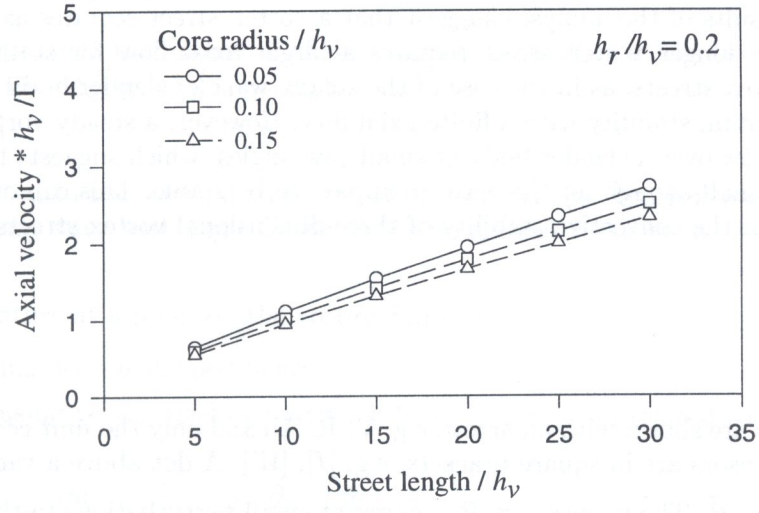

Fig. 4. Minimum axial velocity to maintain stability of vortex street, $h_r/h_v = 0.2$.

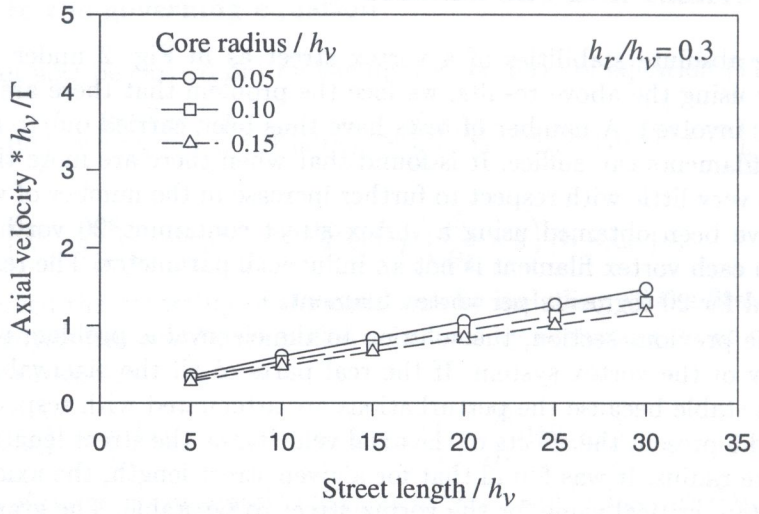

Fig. 5. Minimum axial velocity to maintain stability of vortex street, $h_r/h_v = 0.3$.

The effects of the spacing ratio can be seen by comparing the three graphs (Fig. 3 to 5). Obviously by increasing the spacing ratio, i.e. by having a larger distance between the two rows of vortices. For a given spacing ratio, it is clear that a longer vortex street requires a larger axial velocity to keep it stable. It should be noted at this point that Von Karman found that a two-dimensional vortex street subject only to two-dimensional disturbance can only achieve neutral stability at a spacing ratio of 0.28 [7]. Our analyses suggest that a three-dimensional vortex street subject to three-dimensional disturbance cannot be stable unless an axial flow is present. Here, however, we are only discussing about absolute stability. In practice, the disturbance may grow very slowly, which may appear to look stable.

It can also be seen from these graphs that the effect of the core radius is not very strong, though not negligible. A small core radius tends to have a small destabilising effect which then requires a larger axial velocity to maintain stability.

9. Conclusions

In this paper the principals of the formulation for the analysis of the absolute stability of a finite length vortex street with external axial velocities have been developed using a vortex dynamics algorithm. The results of the analyses suggest that a vortex street requires axial flow to maintain its stability and a longer vortex street requires a larger axial flow for stability. In the case of infinitely long vortex streets, as in the case of the steady wake of slender body flows, it is therefore impossible to maintain stability with a finite axial flow. However, a steady vortex-street type wake does exist in the flow over a slender body at small yaw angles, which suggests that the growth rate of disturbance is small enough for the wake to appear to be stable. This can only be confirmed by the investigation of the convective stability of three-dimensional vortex streets, which is currently underway.

Notations

Vectorial variables are shown with an arrow, e.g. $\vec{V}$, $\vec{R}$. All and only the *unit vectors* are shown with a hat, e.g. $\hat{s}$, $\hat{n}$. Tensors are in square brackets, e.g. $[I]$, $[W]$. A dot above a variable represents the time derivative, e.g. $\dot{\vec{R}}$. The primes, e.g. $\dot{\vec{R}}'$, represent small perturbations to the variable. Symbols not in the following list are defined when they appear.

a Vortex core radius.

$\vec{\mathrm{b}}$ $= \hat{\mathrm{s}} \times \hat{\mathrm{n}}$.

d Cut-off distance.

h_r Distance between the two rows of vortices in a vortex street.

h_v Distance between two vortices on the same row of a vortex street.

$[I]$ Unit tensor.

ℓ_n The length of the n^{th} vortex segment.

$\hat{\mathrm{n}}$ Unit vector pointing from a point on a vortex filament to the local centre of curvature.

$\vec{\mathrm{q}}$ Numerically approximated curvature vector ($\sim \hat{\mathrm{n}}/\rho$).

$\vec{\mathrm{R}}$ Position vector of a point on a vortex filament (time-dependent).

$\hat{\mathrm{s}}$ Unit vector tangential to a point on a vortex filament.

s Curvilinear coordinate of a point on a vortex filament, measured along the vortex. Hence $\partial\hat{\mathrm{s}}/\partial s$ is a vector which points to the centre of curvature at that point, with magnitude equal to the curvature.

T_0 Tension term, occurs when the filament is curved. The swirling flow around the core is distorted and the flow velocities are slightly increased on the concave side and slightly decreased on the convex side of the filament. The resultant changes in the pressure field cause a force, $T_0\hat{\mathrm{n}}/\rho$, on the vortex towards the centre of curvature.

$\vec{\mathrm{V}}_E$ Velocity induced at a point on a vortex filament by all the other vortices.

$\vec{\mathrm{V}}_I$ Velocity induced at a point on a vortex filament by the vortex itself.

v, w Flow velocities in the tangential and axial directions respectively. $\overline{v^2}$, $\overline{w}$ and $\overline{w^2}$ refer to the mean of these quantities calculated over the cross-section of the vortex core.

W Weighting function.

$[W]$ Tensorial weighting function.

α Upwinding factor.

$[\alpha]$ Tensorial upwinding factor.

Δ as in $(\Delta\vec{\mathrm{R}})_n$ represents the difference of the values of a quantity at the two nodes of a vortex segment such that $(\Delta\vec{\mathrm{R}})_n = (\vec{\mathrm{R}}_{n+1} - \vec{\mathrm{R}}_n)$.

Γ Vortex strength.

λ Parameter related to the internal structure of the vortex core, which is a constant along the filament, but may vary with time. If the core has uniform vorticity, $\lambda = \frac{1}{4}$. For details, see reference [4].

ρ Radius of curvature at a point on the vortex filament.

τ Torsion of the filament as defined below.

It can be shown using vector algebra that $\vec{\mathrm{R}}$, $\hat{\mathrm{s}}$, $\vec{\mathrm{b}}$, $\hat{\mathrm{n}}$, τ, and ρ are related to each other in the following equations:

$$\frac{\partial\vec{\mathrm{R}}}{\partial s} = \hat{\mathrm{s}};\ \frac{\partial\vec{\mathrm{b}}}{\partial s} = -\tau\hat{\mathrm{n}};\ \frac{\partial\hat{\mathrm{n}}}{\partial s} = -\frac{\hat{\mathrm{s}}}{\rho} + \tau\vec{\mathrm{b}};\ \frac{\partial\hat{\mathrm{s}}}{\partial s} = \frac{\hat{\mathrm{n}}}{\rho}$$

REFERENCES

[1] T.W. Chiu, L.C. Squire. An Expermental Study of the Slow over a Train in a Crosswind at Large Yaw Angles up to 90°. *J. Wind Eng. & Ind. Aerodyn.*, **45**: 47–74, 1992.

[2] D. Degani, G.G. Zilliac. Experimental Study of Nonsteady Asymmetric Flow around an Ogive Cylinder at Incidence. *AIAA Journal*, **28**(4): 642–649, 1990.

[3] G.G. Zilliac, D. Degani, M. Tobak. Asymmetric Vortices on a Slender Body of Revolution. *AIAA Journal*, **29**(5): 667–675, 1991.

[4] D.W. Moore and P.G. Saffman. The Motion of a Vortex Filament with Axial Flow. *Transactions of the Royal Society of London*, **272**: 403–429, 1972.

[5] A.H. Berney, T.W. Chiu and C.J. Baker. Inverstigation of the Stability of the Vortex Wake Behind a Slender Body at Yaw using a Combined Boundary Element and Vortex Dynamics Algorithm. *Proceedings of the International Conference on Numerical Method in Continuum Mechanics*, 9–16, High Tatras, Slovakia, 19–22 September, 1994.

[6] O.C. Zienkiewicz and R.L. Taylor. *The Finite Element Method*, 4th ed., vol 2, 539–541. McGraw-Hill, London, 1991.

[7] L.M. Milne-Thomson. *Theoretical Hydrodynamics*. MacMillan & Co Ltd, London, 1962.